Daily changes in global cloud cover and Earth transits of the heliospheric current sheet

Article (Accepted Version)

Daily changes in global cloud cover and Earth transits of the heliospheric current sheet

By D.R. Kniveton[1] and B.A. Tinsley[2]

[1] University of Sussex, Falmer, Brighton, BN1 9QJ, UK

[2] University of Texas at Dallas, Richardson, TX, USA

Abstract

Changes in cloud cover are found to occur for periods of a few days following Earth transits of the heliospheric current sheet (HCS), provided also that the transits occur in years of high stratospheric aerosol loading. Using global cloud products from the International Satellite Cloud Climatology Project (ISCCP) D1 data series, epoch superposition analyses was made for various samples of HCS events. For the period August 1991 to June 1994 for the stratospheric aerosol loading due to the Pinatubo eruption, the analysis of the data in 30° geomagnetic latitude intervals revealed that cloud anomalies that were significant and negative were located in the southern hemisphere high and middle latitudes, and anomalies that were significant and positive were found in both hemispheres at low latitudes. When the key days in the superposed epoch analysis were determined by minima in the relativistic electron flux, rather than by the HCS crossings, the location of the significant negative anomalies was in the northern high latitudes, and the location of the significant positive anomalies was in middle latitudes in the northern hemisphere. The spatial and temporal patterns of these cloud cover

variations are in broad agreement agree with the expected opposite variations at high and low latitudes of the current density (Jz) in the global electric circuit caused by the relativistic electron flux variations, during periods when the aerosol loading has made a large increase in stratospheric resistivity

1. **Introduction**

While there is a high degree of scientific certainty concerning the impact of greenhouse gases on the climate system there remains much that is uncertain about the contribution from solar activity to variability in the Earth's climate [IPCC, 2001]. In part this has been due to the lack of generally acceptable physical mechanisms for the interaction between solar variability and the terrestrial climate. Broadly speaking three possible mechanisms have been put forward; variations in the total irradiance; variations in the spectral irradiance in the ultraviolet portion of the electromagnetic spectrum; and variations in the solar wind and the flux of energetic particles [Reid 2000]. The last of these mechanisms has proved particularly controversial especially after the studies of Svensmark and Friss-Christensen [1997] and Marsh and Svensmark [2000] in which galactic cosmic rays (GCR) induced changes in cloudiness were proposed as being responsible for a radiative forcing of 1.4 Wm^{-2} over the period 1901-1995. In terms of the relationship between terrestrial climate and solar activity, the solar wind has a strong role in modulating galactic cosmic ray intensity [Yamada et al., 1998].

A number of reassessments of the findings of Svensmark and Friss-Christensen [1997] and Marsh and Svensmark [2000] by Farrar, [2000]; Jorgensen and Hansen, [2000]; Kernthaler et al., [1999]; Kristijansson and Kristiansen, [2000]; and Sun and Bradley, [2002] have been subsequently undertaken. These studies have raised doubts about the longer-term stability of the cloud-GCR relationship and suggested that the observed variability in cloud cover may be related to the internal climate mechanisms of El Nino-Southern Oscillation and volcanic activity rather than GCR variability. Evidence from century long surface based observations have added to the confusion over the proposed linkage between cloud and GCR, and its consequences to the climate. These observations have suggested that while large uncertainties exist over surface reports of changes in cloud amount over sub-tropical and tropical land areas as well as oceans, total cloud cover appears, contrary to expectations from a GCR-cloud cover link, to have increased since the beginning of the 20th Century, particularly over the mid-to high latitude land areas [IPCC, 2001; Palle and Butler, 2001; Palle and Butler, 2002].

Instead of examining changes in cloud cover over interannual timescales Todd and Kniveton [2001] choose to focus their research into the effect on cloud of short-term Forbush decreases in GCR   The advantage of this is that there is no known natural internal modes of climate variability that operate with similar temporal characteristics as Forbush decrease events. The results of Todd and Kniveton [2001] indicated a highly specific response in the cloud data. Substantial decreases in the highest level cloud (10-180mb) immediately following the onset of Forbush decrease events were observed over the polar latitudes especially in the Southern Hemisphere (SH). Physical explanations for a link between galactic cosmic rays and cloudiness have been based around cosmic ray ionisation related direct and indirect impacts on cloud microphysics [Dickinson, 1975; Tinsley and Deen, 1991; Tinsley and Yu, 2003]. It has been suggested that GCR may directly influence cloud through the production, via cosmic ray ionisation, of cloud condensation and/or ice nuclei. This includes the process known as ion-mediated nucleation [Yu, 2002]. Indirect mechanisms include modulation of the atmospheric electrical conductivity within the GEC by GCR ionisation and subsequent effects on cloud microphysics through the process of electro-scavenging [Tinsley et al., 2000]. In the Tinsley et al., [2000] broad conception of the GEC, the ionosphere-earth current density (Jz) is modulated not only by the solar wind controlled GCR, but also solar wind related relativistic electron precipitation flux, solar proton precipitation, and the polar cap ionospheric convection potentials [Tinsley, 2000].

It should be noted that while laboratory evidence exists of altered microphysical processes due to changes in space charge there is no direct evidence of these processes being observed in the atmosphere [Carslaw et al., 2002]. However there is agreement in onset and duration on the day-to-day timescale between various solar wind modulated parameters and individual tropospheric responses which have hinted at atmospheric temperature and dynamics changes due to Jz related changes in clouds and precipitation [Wilcox, 1979; Page, 1989; Mansurov et al., 1974; Roberts and Olsen, 1973]. In this paper we reassess one of the tropospheric responses, the ‘Wilcox effect’, in terms of cloud cover from satellite data.

The ‘Wilcox effect’ [Wilcox et al., 1973; Hines and Halevy, 1977] involves a decrease in the vorticity area index (VAI) in the middle troposphere in the first and second days following the transits of solar wind magnetic sector boundaries (now known as the heliospheric current sheet or HCS) over the Earth. As a measure of the area covered by values of absolute vorticity above a certain threshold, the VAI can be considered an objective measure of the intensification of cyclonic storms and the deepening of low-pressure troughs [Tinsley et al., 1994]. It should be noted that HCS transits have never been regarded as atmospheric forcing agents in themselves, but rather as convenient markers (that can be detected in ground as well as spacecraft magnetic signatures) for other changes in the solar wind or space weather.

The HCS is the warped surface that at minimum solar activity lies approximately in the equatorial plane of the sun. During a given 11-year period between successive solar maxima the interplanetary magnetic field is directed away from the sun in one hemisphere, say the northern helio-hemisphere, while towards it in the other. This pattern reverses after each solar maximum, following the 22-year Hale cycle of solar magnetic polarity. The boundary between the outward and inward field lines was first detected by Wilcox and Ness [1965] from observations with the Imp 1 spacecraft. The boundary is formed by a current sheet that is warped like a ballerina skirt due to the interplay of the large scale solar magnetic field and the irregularities in the active region distribution at lower solar latitudes [El-Borie, 1999]. It generally follows the similarly warped region of low speed solar wind [Zhao and Hundhausen, 1983] that is the extension of the low-latitude coronal streamer belt. As the sun rotates, so does the warped low-velocity region and current sheet, and they pass over the Earth two, four, six or more times each 27-day solar rotation period.

The Earth transits of the low velocity region can begin several days before the HCS transit, and the minimum of velocity has been suggested to be within one or two days of the HCS transit [Tinsley et al., 1994]. The energization of a relativistic electron flux (REF) in the Earth's radiation belts, and precipitation of a REF from them is dependent on the solar wind velocity [Li et al., 2001a,b]. Observations show that GCR changes, as recorded by neutron monitors, are not systematically associated with transits of the HCS [Laštovicka, 1987, Tinsley et al., 1994], but that there are systematic reductions in precipitating REF. It has been suggested that the REF precipitation generates Bremsstrahlung X-rays that cause conductivity changes in the middle stratosphere, and that these may modulate the current density (Jz) of the GEC [Tinsley et al., 1994; Kirkland et al., 1996]. There are only sparse and noisy data on the Jz variations near HCS crossings but these have shown reductions for periods of relatively high stratospheric aerosol loading [Park, 1976; Reiter, 1977; Tinsley et al., 1994, based on data of Fischer and Mühleisen, 1980]. Periods of high stratospheric aerosol loading occurred in 1963-70, 1982-86, and 1991-94, as illustrated, for example, in Sato et al. [1993, Fig. 1].

After the initial citing of the Wilcox effect subsequent studies showed that the amplitude varied, decreasing in the late 1960s and early 1970s before falling below the noise level after 1974 [Williams and Gerety, 1978; Shapiro, 1979]. In common with many other nonstationary statistical climate/solar relationships this prompted claims that the phenomenon was merely a chance coincidence. However the original observations of the effect were in the period of enhanced stratospheric aerosol loading following the explosive volcanic eruption of Agung in 1963 and some smaller eruptions several years later. A reappearance of this effect following the eruption of El Chichon in 1982, and again following Pinatubo in 1991 re-ignited interest in the Wilcox effect. Tinsley et al. [1994] and Kirkland et al. [1996] made the suggestion that increased a stratospheric aerosol loading was a pre-requisite for aerosol loading was a pre-requisite for changes in the global circuit that modify cloud microphysics and cause this effect to occur. The idea that volcanic eruptions can influence solar-climate relationships was pursued by Donarummo et al., [2002] who examined the relationship between the Greenland Ice Sheet Project 2 dust profile and Wolf sunspot number from 1752 to 1988. Their work suggested that while the two records are positively correlated, the effects of volcanic eruptions had disturbed the phase of the relationship.

In this study we aim to quantify changes on global and regional patterns of cloud cover prior, during and after HCS events. As part of this we intend to evaluate the sensitivity of the results to variations in precipitating REF and the presence of stratospheric volcanic aerosols.

2. Data and Method

The International Satellite Cloud Climatology Program (ISCCP) produces the currently most comprehensive database of global cloud cover. A range of cloud parameters is available from ISCCP, for every 3 hours on a 2.5° latitude-longitude grid [Rossow et al., 1996]. For this study we have selected eight variables from the 1987-1994 period of the ISCCP dataset, D1 (Table 1). The methodology used in this study is the 'epoch superposition' analysis, as used in previous studies of this kind (see Todd and Kniveton, 2001). The method relies on selecting a sample of key dates and extracting ISCCP D1 data for the period 5 days prior to 5 days following each date. The cloud parameters are then averaged over the sample for each time slot (day –5 to day 5) separately. This is akin to compositing routinely used in climate analysis. The difference between conditions prior to, during and after the key days can then be established by subtracting the mean values at different time slots. Here, we define a 'base period' sample representative of conditions prior to an event as the mean of days –5 to –3. The mean cloud values at all days from day –5 to day 5 are then derived and from this the anomaly is obtained by subtracting the mean of the base period. The result is tested for local statistical significance using a t-test at the 0.05 probability level. Throughout, the anomalies are given as absolute values rather than as a percentage of the base period value.

Key dates of Earth transits of the HCS were taken from Kirkland et al. [1996] (following Svalgaard, 1979), where the Earth transit of the HCS is characterized by a persistent reversal of the ambient interplanetary magnetic field (IMF) polarity. Particular key dates were taken from measurements by magnetometers of the B_y component of the IMF [see Kirkland et al., 1996]. Kirkland et al., [1996] found that the Earth transits of the HCS occurred during periods of decreases in the mean REF measured at satellite altitude (a proxy for the precipitating flux). These periods also were when the low velocity solar wind is encountered, as discussed earlier.

In Figure 1a the mean change in REF for the HCS dates between September 1986 and May 1994 is shown, as well those for HCS dates during 1987 (near solar maximum) and 1991 (near solar minimum). While the mean pattern shows a decrease in REF at HCS key dates followed by a rise, this is not uniformly true with the REF sometimes increasing on the key date, or not changing relative to the prior days. Additionally it can be seen from Figure 1b and Figure 1c that the magnitude of REF changes at earth transits of HCS also varies inter-annually.

To test the extent to which changes in cloud near HCS dates were directly related to changes in the precipitation REF, (as opposed to say some other statistically related space weather parameter) a list of key dates were derived when the REF, as measured by the Space Environment Monitor (SEM) package on the GOES 7 satellite, fell in a similar manner to that during HCS events. In order to define a REF key event a moving 14-day window was used to first determine the dates of minimums in the REF data. Where a number of minimum dates were close to each other (defined as not separated by at least 5 days) the minimum date chosen for further consideration was the one that was the lowest before the REF increased. Further filtering of these dates was achieved by limiting the minimum dates to days when the REF count on the key date and that the two days following a key date were all less than the count on dates five, four and three days prior to a key date. This was done to ensure that the dates collected were sustained drops in the REF. The rule for defining a ‘REF key day’ during HCS events, i.e., when the REF dropped during a HCS event, was if the REF decreased on the key date below the REF values on the dates, three, four and five days prior to the key event. A list of these key dates is shown in Table 2. It should be noted that these dates are not all independent of HCS crossing times with 5 of the 32 events being on the same days as HCS events. Unfortunately the electron detector on GOES responds significantly to protons with energies above 32 MeV, including solar protons and galactic cosmic ray protons. This means that electron fluxes are evaluated from the satellite data as a flux that may include protons of energy > 32 MeV. Large increases in the solar proton flux are easily recognized and are flagged accordingly. Any effects of smaller changes are discussed in Section 4. This means the electron data are contaminated when a proton event occurs, and are flagged accordingly (NASA). Lastly key HCS and REF dates were separated according to whether they occurred when the stratospheric volcanic aerosol loading was high and when it was not. Table 3 lists the different experiments on cloud cover, the assumptions behind calculating the key dates and the period for which they were calculated. The period over which the key dates were included in the analysis, was decided from the availability of the different datasets.

3. Results

Figure 2 shows the mean percentage coverage of cloud during the base period day –5 to –3 for Experiments 1 (see Table 3). The structure of cloud cover for all experiments (not shown) are in very close agreement both in terms in absolute and relative cloud amounts with the long-term average cloud conditions determined from the ISCCP D2 dataset

[Rossow and Schiffer, 1999]. From this we are confident that our sample of events is representative of the long-term climatology, providing evidence that our sample size is large enough to highlight any systematic changes in cloud cover associated with earth transits of HCS and REF decrease events.

Much of the theory on the interaction of solar wind related phenomena and cloud suggests a geomagnetic latitudinal (φ) dependence of these processes, due to the strong role the Earth's magnetic field plays in modulating the various fluxes. Accordingly, cloud anomalies were also derived in 30° φ (hereinafter referred to simply as 30° latitude) bands. The mean anomalies of 30° latitude band averaged values of total cloud cover (cloud variable 1 in Table 1) over both land and sea surfaces for all experiments are shown as contours in Figures 3 (a-h) as a function of geomagnetic latitude (abscissa) and day number (ordinate) for day numbers –5 to +5 relative to the key day (day 0). Statistically significant (at 95% significance level, and hereinafter simply referred to as statistically significant) positive anomalies are present in the period two days prior to two days post key date, in Experiments 2 at 0-30ºS, Experiment 6 at 0-30ºS and 0-30ºN and Experiment 8 at 30-60ºN, while significant negative anomalies are present in Experiment 4 at 60-90ºS, Experiment 6 at 60-90ºS and 30-60ºS and in Experiment 8 at 60-90ºN.

The mean anomalies of 30° latitude band averaged values of cloud cover at different altitudes in the atmosphere (cloud variables 2-8, in Table 1) over both land and sea surfaces for Experiments 6 and 8 are shown as contours in Figures 4 (a-g) and 5 (a-g), respectively, as a function of geomagnetic latitude (abscissa) and day number (ordinate) for day numbers –5 to +5 relative to the key day (day 0). Statistically significant positive anomalies are present in the period two days prior to two days post key date, in low altitude clouds for Experiments 6 at 0-30ºN and 30-60ºN, and in high altitude clouds for Experiment 8 at 30-60ºN, while significant negative anomalies are present in high altitude clouds in Experiment 6 at 30-60ºN and 60-90ºN, and in Experiment 8 at 60-90ºN.

4. Discussion and conclusion

Of the physical mechanisms put forward to explain the potential coupling between solar variability and climate, variations in the solar wind and the flux of energetic particles, has tended to be the most controversial. In this paper we have examined the variations in latitudinal cloud cover coincident with one of the manifestations of variation in the solar wind; Earth transits of the heliospheric current sheet. As shown above, on average, earth transits of the HCS coincide with a decrease in relativistic electron flux. While relativistic electrons do not penetrate to the troposphere, they do reach the stratosphere at high latitudes and thus it has been suggested that, in theory, they should alter the stratospheric column resistance in the GEC [Tinsley, 2000]. Considered relatively insignificant, compared to the tropospheric resistance, the stratospheric column resistance to current density would be expected to increase when the stratospheric aerosol loading is relatively high following a large volcanic eruption.

During periods of high stratospheric resistance, ionization produced by relativistic electron precipitation in a given region would be expected to reduce the column resistance in that region to levels comparable to that in the absence of volcanic aerosols.

However, temporary decreases in the electron flux during such periods, coincident with an Earth transit of the HCS, would then be expected to temporarily increase the stratospheric column resistance at high latitudes. In turn, this would temporarily decrease the current density, Jz, flowing from the ionosphere through clouds to the surface. The few sparse and noisy observations of Jz support this scenario [Tinsley et al, 1994]. The linkage with cloud cover comes from some combination of the proposed cloud microphysical processes of ion-mediated nucleation and electroscavenging driven by the current density [Tinsley and Yu, 2003]. While it is not the purpose of this paper to evaluate mechanisms, we will outline two possibilities, while not excluding others. Firstly, in the cloud environment (as opposed to clear air) the flow of Jz through local gradients of conductivity generates space charge. Reductions in Jz cause reductions in positive space charge at cloud top, and reductions in negative space charge at cloud base. Space charge can stabilize charged clusters against recombination, so decreases can decrease production of ultrafine aerosols and their growth to CCN, from positive ions at cloud top or negative ions at cloud base. The reduction in CCN reduces cloud cover by reducing cloud lifetime by the indirect aerosol effect [Tinsley and Yu, 2003].

The second possibility related to the reduction in space charge is that it can either decrease or increase scavenging of CCN, depending on the size of the CCN and the size of the droplets. The charges on the particles and droplets in the presence of space charge will be proportional to the space charge density, and predominantly of like sign. From the results of Tinsley et al. [2001, Figure 2a] for electroscavenging on droplets of radius 7 μm, and in the presence of Brownian or phoretic scavenging, a decrease in the charge on particles and droplets increases the scavenging of CCN less than about 0.12 μm diameter, and decreases the scavenging of CCN greater than about 0.3 μm diameter. For a typical oceanic aerosol spectrum [e.g. Pueschel et al., 1994] the net effect could be an decrease in CCN concentration and a broadening of their size distribution, with consequences similar to those discussed above for the decreased production from ultrafines.

If one considers the GEC to be comprised of return paths at high and low latitudes in parallel, as a load on a constant current source [Tinsley, 1996] then the increase in column resistance at high latitudes would be expected to increase current density at low latitudes and cause opposite changes in cloud cover there. If the GOES nominally electron flux data are also responding to decreases in the proton flux above 32 MeV at HCS crossings, the decreases in these will produce increases in stratospheric column resistance and decreases (increases) in Jz at high (low) latitudes, as illustrated by Sapkota and Varshneya [1990, Fig. 14]. With opposite changes in Jz at low as compared to high latitudes, one would expect opposite cloud cover changes also.

If the GOES measurements of nominally electron flux decreases include responses to decreases in the proton flux above 32 MeV at HCS crossings, these will produce similar increases in stratospheric column resistance, and thus on Jz and cloud cover, so the ambiguity in identification is not so important. As noted in the Introduction, the neutron monitor measurements of cosmic ray proton fluxes above about 2000 MeV do not show systematic decreases at HCS crossings.

The results presented here show no statistically significant cloud cover anomalies when all HCS dates are considered for the period 1987-1994. However when the HCS dates are separated according to whether they occur in years of high or low stratospheric aerosol loadings a statistically significant anomaly appears at 0-30ºS on the day following the key date, in years with a high stratospheric aerosol loading. No significant cloud anomalies are apparent in years of low stratospheric loading. When the HCS dates are sorted by whether the relativistic flux decreases on the key date and two days following it, a statistically significant negative anomaly appears at 60-90ºS on the key date. No statistically significant anomalies occur when only dates are included where the REF does not decrease. Further sub-sampling of the HCS dates to include only dates when there is a high stratospheric aerosol loading and a sustained drop in the relativistic electron flux highlights statistically significant negative cloud anomalies at high latitudes of 60-90ºS and positive anomalies at low latitudes of 0-30ºS and 0-30ºN on the key date. On the day following the key date the positive anomalies are still present at low latitudes and are joined by a significant negative anomaly at 30-60ºS. These results seem consistent with the above conception of the role of changes in the relativistic electron flux in affecting the GEC. However it should be pointed out with the exception of the statistically significant positive anomaly at 0-30º, no significant anomalies are present in the northern hemisphere and while there is a drop in cloud cover at 60-90ºN, there is actually an increase in cloud cover at 30-60ºN. If we look at the cloud anomalies on the key date (Figure 6) we see that the pattern of decreased cloud cover at high latitudes and increased cloud cover at low latitudes is present in both hemispheres.

The breakdown of anomalies by altitude reveals that the statistically significant negative (positive) anomalies are confined to high (low) altitude clouds at high and middle (low and middle) latitudes. However it should be noted that these anomalies are confined to the northern hemisphere. Finally it should be remembered that the sample size for Experiment 6 is small, only 21 events.

Turning to the experiments using only the REF data to determine key dates and limiting them to years when the stratospheric aerosol loading is high no statistically significant anomalies are present in the southern hemisphere. Instead significant negative anomalies are present at 60-90ºN and positive ones at 30-60ºN. Thus, while there is agreement between the cloud cover changes on REF and HCS defined dates that there is a decrease at high latitudes in cloud cover there is not a consistent pattern of increased cloud cover at low latitudes and an apparent asymmetry of response between the northern and southern hemispheres at mid-latitudes. In part, the lack of coherence in response between the two types of sampling could be due to the inability of the definition used to pick REF dates, to select HCS type decreases in REF. Also, the REF is measured at one local time, and may not be as representative of all local times as the HCS crossings. Alternatively the difference may indicate that changes in REF are only one of several variable affecting cloud cover at Earth transits of the heliospheric current sheet. The breakdown of anomalies by altitude reveals fewer statistically significant anomalies than observed in Experiment 6 of the HCS dates, with negative anomalies only observed at high latitudes and with high altitude cloud, and positive anomalies observed in the higher altitude clouds at middle latitudes. Again statistically significant results are limited to the northern hemisphere.

The possibility that short-term dynamical changes occur in the troposphere in response to solar UV changes was raised by Gabis and Troshichev [2000]. We do not consider that UV variations are a plausible candidate to explain the present cloud cover changes associated with HCS crossings because solar UV is absorbed in the stratosphere, and the time constant for dynamic coupling to the troposphere is weeks to months [Perlutz and Graf, 2001; Kuroda and Kodera, 2001;Thompson and Solomon, 2002; Gillet and Thompson, 2003], whereas the phase lag for the present results is less than a the order of a day (as expected for electrical coupling via the GEC).

Therefore we tentatively conclude that cloud cover observations, during HCS events when the stratospheric aerosol loading is high and the relativistic electron flux declines, concur with the expected behavior of the Global Electric Circuit proposed by Tinsley [1996]. However it is noted that when selecting key dates using purely the relativistic electron flux the evidence for a Global Electric Circuit based explanation of cloud cover changes is not as strong. In particular, the disparity in results between the HCS and REF based experiments at low latitudes raises the possibility that the changes being seen at Earth transits are not purely related to changes in the relativistic electron flux. Further research is required related to changes cloud cover coincident with variations in the relativistic electron flux.

Lastly as with all empirical studies of this kind there are a number of caveats that must be noted when considering the conclusions drawn here. First, given the complexity of solar-atmosphere relations there remains, other possible physical explanations of observed changes in cloud cover, not discussed in this paper. Second it is possible that because of the satellites view point, cloud amounts at different vertical levels are not truly independent of each other, in that low-level cloud amounts may be inversely related to those at upper levels. An example of this might explain the opposite sign of anomalies shown at middle latitudes in the higher and lower altitude clouds seen in Experiment 6. Thirdly, by assuming linearity and uniformity in the response of the atmosphere to HCS events the methodology of epoch superposition itself may conceal important information on the precise nature of these interactions. Finally it must be remembered that for a number of the experiments (6 and 7) described in this study the sample sizes are particularly small. While the statistical significance testing takes this into account, the recent ISCCP data from 1995-2001 would allow a larger sample size when testing the lack of response at HCS events when the stratospheric aerosol loading is low and this should be studied further. For this study however we feel the conclusions on the role of the stratospheric aerosol loadings are supported by cloud cover responses shown in the larger sample sized Experiments 2 and 3.

Acknowledgements

The authors would like to thank the International Satellite Cloud Climatology Program (ISCCP) and the Goddard Institute for Space Studies for production of the ISCCP data and the Distributed Active Archive Center at Langley Research Center, EOSDIS, for its distribution. These activities are sponsored by NASA's Mission to Planet Earth. We are also grateful to the NOAA National Geophysical Data Center for the relativistic electron flux data. Support for BAT has been provided by NSF grant ATM 9903424.

References

Carslaw K.S., R.G. Harrison and J. Kirkby, Cosmic rays, clouds and climate, *Science*, 298, 5599, 1732-1737, 2002.

Cess, R.D. and P.M. Udelhofen, Climate change during 1985-1999: Cloud interactions determined from satellite measurements. Geophys. Res. Lett., 30 (1): art. no. 1019, 2003.

Dickinson, R.E., Solar variability and the lower atmosphere, *Bull. Amer. Meteorol. Soc*., 56, 1240-1248, 1975.

Donarummo, J. Jr., M., Ram, M.R. Stolz, Sun/dust correlations and volcanic interference, *Geophys. Res. Lett*., 29(9), 75, doi10.1029/2002GL014858, 2002.

El-Borie, M.A., Correlation of the heliospheric current sheet tilts to galactic cosmic ray modulations and solar wind speed. *Astroparticle Physics*, 10 (2-3): 165-174, 1999.

Farrar P.D., Are cosmic rays influencing oceanic cloud coverage-or is it only El Nino? *Climatic Change*, 47 (1-2): 7-15, 2000.

Fischer, H. J., and R. Mühleisen, The ionospheric potential and the solar magnetic sector boundary crossings, Rept. Astronom. Inst. Univ. Tübingen, Ravensberg, Germany, 1980.

Gabis, I.P. and O.A. Troshichev, Influence of short-term changes in solar activity on baric field perturbations in the stratosphere and troposphere, *J. Atmos. & Solar Terr. Phys.,* 62 (9), 725-735, 2000.

Gillet, N. P., and D. W. J. Thompson, Simulation of recent southern hemisphere climate change, *Science*, 302, 273-275, 2003.

Hines C.O., and I. Halevy, On the reality and nature of a certain sun-weather correlation, *J. Atmos. Sci*., 34, 382, 1977.

IPCC, *Climate Change 2001: The scientific Basis. Contibution of Working Group I to the third Assessment Report of the Intergovernmental Panel on Climate Change* [Houghton, J.T., Y. Ding, D.J. Griggs, M. Noguer, P.J. van der Linden, X. Dai, K. Maskell, and C.A. Johnson (eds.)]. Cambridge University Press, Cambridge, United Kingdom and New York, NY, USA, 881pp, 2001.

Jorgensen T.S., and A.W. Hansen, Comments on "Variation of cosmic ray flux and global cloud coverage - a missing link in solar-climate relationships" by Henrik Svensmark and Eigil Friis-Christensen [Journal of Atmospheric and Solar-Terrestrial Physics 59 (1997) 1225-1232], *J. Atmos. & Solar Terr. Phys., 62,* 73-77, 2000.

Kernthaler S.C., R. Toumi and J. Haigh, Some doubts concerning a link between cosmic ray fluxes and global cloudiness, *Geophys. Res., Lett., 26,* 863-865, 1999.

Kirkland, M., B.A. Tinsley, J.T. Hoeksema, Are stratospheric aerosols the missing link between tropospheric vorticity and Earth transits of the heliospheric current sheet?, *J. Geophys. Res*., 101, 29,689 - 29,699, 1996.

Kuroda, Y., and K. Kodera, Variability of the polar night jet in the northern and southern hemispheres, J. Geophys. Res., 106, 20,703-713, 2001.

Kristjansson J. E., and J. Kristiansen, Is there a cosmic ray signal in recent variations in global cloudiness and cloud radiative forcing, *J. Geophys. Res*., 105, 11851-11863, 2000.

Li, X., M. Temerin, D.N. Baker, G.D. Reeves and D. Larson, quantitative prediction of radiation belt electrons at geostationary orbit based on solar wind measurements, Geophys. Res. Lett., 28, 1887-1890, 2001a.

Li, X., D.N. Baker, S.G. Kanekal, M. Looper and M. Temerin, Long term measurements of radiation belts by SAMPEX and their variations, Geophys. Res. Lett., 28, 3827-3830, 2001b.

Mansurov, S.M., L.G. Mansurova, G.S, Mansurov, V.V. Mikhenvich, and Visotsky, A.M., North-south asymmetry of geomahnetic and tropospheric events, *J. Atmos. Terr*. Phys. 36, 1957-1962, 1974.

Marsh, N. and H. Svensmark, Low cloud properties infuenced by cosmic rays, *Phys. Rev. Lett.*, 85, 5004-5007, 2000.

Park, C.G., Solar magnetic sector effects on the vertical atmospheric electric field at Vostok, Antartica, *Geophys. Res. Lett.* 3, 475-478, 1976.

Palle, E., and C.J. Butler, Sunshine, clouds and cosmic rays, in Proceedings of the first SOLSPA, *Euroconference*, Canary Islands, September, 2000.

Palle, E., and C.J. Butler, The influence of cosmic terrestrial clouds and global warming. *Astronomy & Geophysics*, 41(4), 8-22. 2000.

Perlutz, J., and H.-G. Graf, Tropospheric – stratospheric dynamic coupling under strong and weak polar vortex conditions, *Geophys. Res. Lett*., 28(2), 271-274, 2001.

Reid, G.C., Solar variability and the Earth's climate: Introduction and overview, Space Science Reviews, 94 (1-2), 1-11, 2000.

Pueschel, R. F., J.M. Livingston, G.V. Ferry and T.E. DeFelice, Aerosol abundances and optical characteristics in the Pacific basin free troposphere, *Atmos. Env.,* 28(5), 951-960, 1994.

Reiter, R., The electric potential of the ionosphere as controlled by the solar magnetic sector structure; result of a study over the period of a solar cycle, *J. Atmos. Terr. Phys.,* 39, 95-99, 1977.

Roberts, W.O., and R.H. Olsen, Geomagnetic storms and wintertime 300mb trough development in the North Pacific-North America area, *J. Atmos. Sci.,* 30,135, 1973.

Rossow, W. B., and R.A. Schiffer, Advances in understanding of clouds from ISCCP. *Bull Amer. Meteor. Soc*., 80, 2261-2287, 1999.

Rossow, W. B., A.W. Walker, D.E. Beuschel, and M.D. Roiter, ISCCP documentation of new cloud datasets. WMO Tech. Document 737, 115pp,World Climate Research Program, Geneva, Switzerland, 1996.

Sapkota, B. K., and N. C. Varshneya, On the global atmospheric electrical circuit, J. Atmos. Terr. Phys., 52, 1-20, 1990.

Sato, M., J. E. Hansen, M. P. McCormic and J. B. Pollak, Stratospheric aerosol optical depths, 1850-1990, *J. Geophys. Res.*, 98(D12), 22,987 – 22,994, 1993.

Shapiro, R., An examination of a certain proposed sun-weather correlation. *J. Atmos. Sci*., 36, 1105-1116, 1979.

Sun, B.M., and R.S. Bradley, Solar influences on cosmic rays and cloud formation: A reassessment. *J. Geophys. Res.,* 107 (D14): art. no. 4211, 2002.

Svalgaard, L., Solar Sector Boundary Crossings, 1975-78, in *Solar Terrestrial Physics and Meteorology: Working Document III*, complied by A.H. Shapley, C.D. Ellyett, and H.W. Kroehl, 107p, SCOSTEP, Boulder, Colo., 1979.

Svensmark, H., and E. Friis-Christensen, Variation of cosmic ray flux and global cloud coverage – A missing link in solar-climate relationships. *J. Atmos. & Solar Terr. Phys*. 59 1225-1232, 1997.

Thompson, D. W. J., and S. Solomon, Interpretation of recent southern hemisphere climate change, *Science*, 296, 895-899, 2003.

Tinsley, B. A., and G. W. Deen, Apparent tropospheric response to MeV-GeV particle flux variations: A connection via electrofreezing of supercooled water in high level clouds? *J. Geophys. Res*.**,** 96, 22283-22296, 1991.

Tinsley, B. A., J.T. Hoeksema, and D.N. Baker, Stratospheric volcanic aerosols and changes in air-earth current density at solar wind magnetic sector boundaries as conditions for the Wilcox tropospheric vorticity effect, *J. Geophys. Res.*, 99, 16,805 - 16,813, 1994.

Tinsley, B. A., Correlations of atmospheric dynamics with solar wind-induced changes of air-earth current density into cloud tops, *J. Geophys. Res., 101,* 29701-29714*,* 1996.

Tinsley, B. A., Influence of the solar wind on the global electric circuit, and inferred effects on cloud microphysics, temperature, and dynamics of the troposphere, *Space Science Reviews*, 94, 231-258, 2000.

Tinsley, B.A., R.P. Rohrbaugh, M. Hei, and K.V. Beard, Effects of image charges on the scavenging of aerosol particles by cloud droplets and on droplet charging and possible ice nucleation processes, *J. Atmos. Sci*., 57, 2118-2134, 2000.

Tinsley, B. A., and F. Yu, Atmospheric ionization and clouds as links between solar activity and climate, in press, Solar Variability and its Effects on the Earth's Atmospheric and Climate System, J. Pap et al. (eds), AGU press, Washington, DC, 2003.

Todd, M.C., and D.R. Kniveton, Changes in cloud cover associated with Forbush decreases of galactic cosmic rays. *J. Geophys. Res*. 106 (D23), 32031-32042, 2001.

Wilcox, J.M., P.H. Scherrer, L. Svalgaard, W.O. Roberts, and R.H. Olsen, Solar magnetic sector structure: Relation to circulation of the Earth's atmosphere, *Science*, 180, 185, 1973.

Wilcox, J.M., Tropospheric circulation and interplanetary magnetic sector boundaries followed by MeV proton streams, Nature, 278, 840-841, 1979.

Wilcox, J. M., and N. F. Ness, Quasi-stationary corotating structure in the interplanetary medium, J. Geophys. Res., 70(23), 5793-5805, 1965.

Williams, R.G., and E.J. Gerety, Does the troposphere respond to day-to day changes in solar magnetic field?, *Nature*, 275, 200, 1978.

Yamada,Y., S. Yanagita and T. Toshida, A stochastic model of the solar modulation phenomena of cosmic rays, *Geophys. Res. Lett*., 25, 2353-2356, 1998.

Yu, F., Altitude variations of cosmic ray induced production of aerosols: Implications for global cloudiness and climate, *J. Geophy. Res*., 107 (A7), art. no. 1118, 2002.

Zhao, X.-P., and A. J. Hundhausen, Spatial structure of the solar wind in 1976, J. Geophys. Res., 88(A1), 451-454, 1983.

Table titles

Table 1. Cloud variables extracted from ISCCP D1 data used in this study. Variables 2-8 are based on thermal infrared data only.

Table 2. List of key dates defined from the REF data (see text for details of definition)

Table 3. Different experiments of cloud changes using key dates, defined in text.

Figure captions

Figure 1(a) Mean variation in relativistic electron flux for earth transits of the HCS from July 1987 to June 1994 (thick line), with +/- one standard deviation of the relativistic electron flux (grey lines), (b) variation in relativistic electron flux as measured by the SEM on GOES 7 for 5 days prior and post HCS events, for the year 1988, (c) variation in relativistic electron flux as measured by the SEM on GOES 7 for 5 days prior and post HCS events, for the year 1992. The ordinate in each figure is the logarithm of the REF count rate.

Figure 2. Mean total cloud percentage coverage during the 'base period' (days –5 to –3 prior to onset of key date) for Experiments 1, where 1 is overcast and 0 is clear sky. Thirty degree geomagnetic latitude bands are also shown by the long white dashed lines.

Figure 3. Zonal mean (averaged over 30 degree geomagnetic latitude bands) total cloud percentage coverage anomalies (relative to base period) for days –5 to 5 for Experiments 1-8 (Figures 3a-h) over both land and sea surfaces. Positive (negative) anomalies have solid (dotted) contours. The contour interval is 0.5% and statistically significant anomalies (at 0.05 probability level) are shaded.

Figure 4. Zonal mean (averaged over 30 degree geomagnetic latitude bands) cloud percentage coverage anomalies (relative to base period) for days –5 to 5 for; (a) pixels defined as level 1 cloud (10-180mb), (b) pixels defined as level 2 cloud (180-310mb), (c), pixels defined as level 3 cloud (310-440mb), (d) pixels defined as level 4 cloud (440-560mb), (e) pixels defined as level 5 cloud (560-680mb), (f) pixels defined as level 6 cloud (680-800mb), and (g) pixels defined as level 7 cloud (800-1000mb), for Experiment 6, over both land and sea surfaces. Positive (negative) anomalies have solid

(dotted) contours. The contour interval is 0.1% and statistically significant anomalies (at 0.05 probability level) are shaded.

Figure 5. Zonal mean (averaged over 30 degree geomagnetic latitude bands) cloud percentage coverage anomalies (relative to base period) for days –5 to 5 for; (a) pixels defined as level 1 cloud (10-180mb), (b) pixels defined as level 2 cloud (180-310mb), (c), pixels defined as level 3 cloud (310-440mb), (d) pixels defined as level 4 cloud (440-560mb), (e) pixels defined as level 5 cloud (560-680mb), (f) pixels defined as level 6 cloud (680-800mb), and (g) pixels defined as level 7 cloud (800-1000mb), for Experiment 8, over both land and sea surfaces. Positive (negative) anomalies have solid (dotted) contours. The contour interval is 0.1% and statistically significant anomalies (at 0.05 probability level) are shaded.

Figure 6. Zonal mean (averaged over 30 degree geomagnetic latitude bands) total cloud percentage coverage anomalies (relative to base period) for the key date, for Experiment 6, over both land and sea surfaces. The lines above and below the mean anomalies denote +/- one standard deviation of the zonal mean total cloud percentage coverage.

Table 1.

Variable	**Description**
1	Proportion of all pixels defined as cloudy
2	Proportion of all pixels defined as level 1 cloud (10-180mb)
3	Proportion of all pixels defined as level 2 cloud (180-310mb)
4	Proportion of all pixels defined as level 3 cloud (310-440mb)
5	Proportion of all pixels defined as level 4 cloud (440-560mb)
6	Proportion of all pixels defined as level 5 cloud (560-680mb)
7	Proportion of all pixels defined as level 6 cloud (680-800mb)
8	Proportion of all pixels defined as level 7 cloud (800-1000mb)

Table 2.

Key date	**Key date**
1991/08/12	1992/12/01
1991/08/20	1992/12/18
1991/09/11	1992/12/28
1991/09/23	1993/01/12
1991/10/20	1993/02/18
1991/11/29	1993/03/01
1991/12/08	1993/03/30
1992/01/02	1993/05/01
1992/02/20	1993/05/28
1992/04/04	1993/06/12
1992/04/19	1993/08/28
1992/04/30	1993/09/24
1992/05/20	1993/10/07
1992/07/28	1993/10/25
1992/09/10	1994/03/21
1992/10/10	1994/04/17

Table 3.

Experiment	**Definition of key dates**	**Period over which key dates defined**	**Sample size**
1	All HCS events as defined by Kirkland et al., [1996]	July 1986 to June1994	123
2	HCS events during high stratospheric volcanic aerosol concentrations	August 1991 to June 1994	46
3	HCS events during low stratospheric volcanic aerosol concentrations	July 1986 to July 1991	77
4	HCS events when the REF decreased relative to that on 3, 4 and 5 days prior.	July 1986 to June1994	39
5	HCS events when the REF did not decrease relative to that on 3, 4 and 5 days prior.	July 1986 to June1994	84
6	HCS events when the REF decreased relative to that on 3, 4 and 5 days prior and there was a high stratospheric volcanic aerosol loading.	August 1991 to June1994	21
7	HCS events when the REF decreased relative to that on 3, 4 and 5 days prior and there was a low stratospheric volcanic aerosol loading	July 1986 to July 1991	18
8	REF dates when there was a high stratospheric volcanic aerosol loading	August 1991 to June1994	32

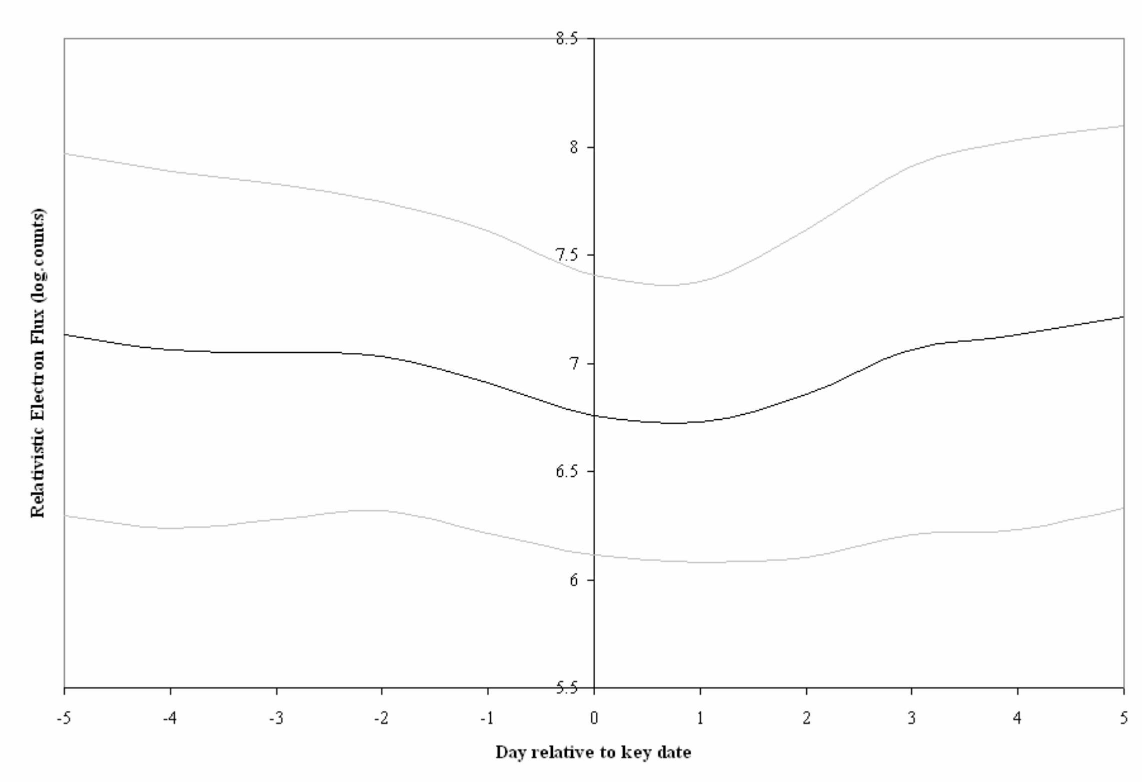

8.5
8
7.5
7
6.5
6
5.5
Relativistic Electron Flux (log.counts)
-5
-4
-3
-2
-1
0
1
2
3
4
5
Day relative to key date

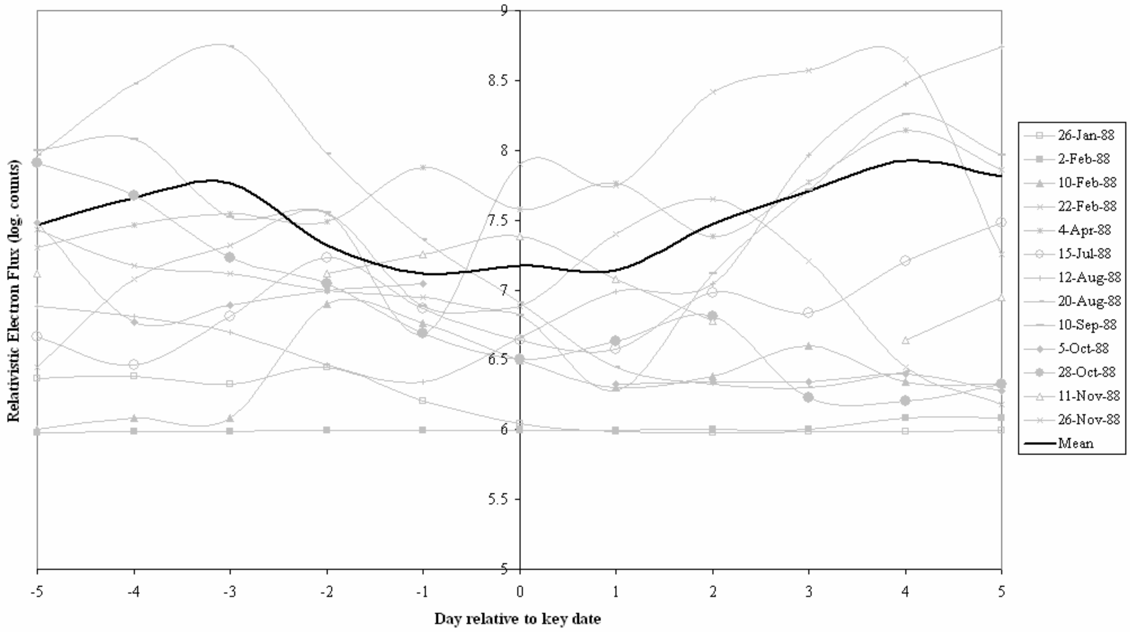

Relativistic Electron Flux (log. counts)
Day relative to key date
9
8.5
8
7.5
7
6.5
6
5.5
5
-5
-4
-3
-2
-1
0
1
2
3
4
5
26-Jan-88
2-Feb-88
10-Feb-88
22-Feb-88
4-Apr-88
15-Jul-88
12-Aug-88
20-Aug-88
10-Sep-88
5-Oct-88
28-Oct-88
11-Nov-88
26-Nov-88
Mean

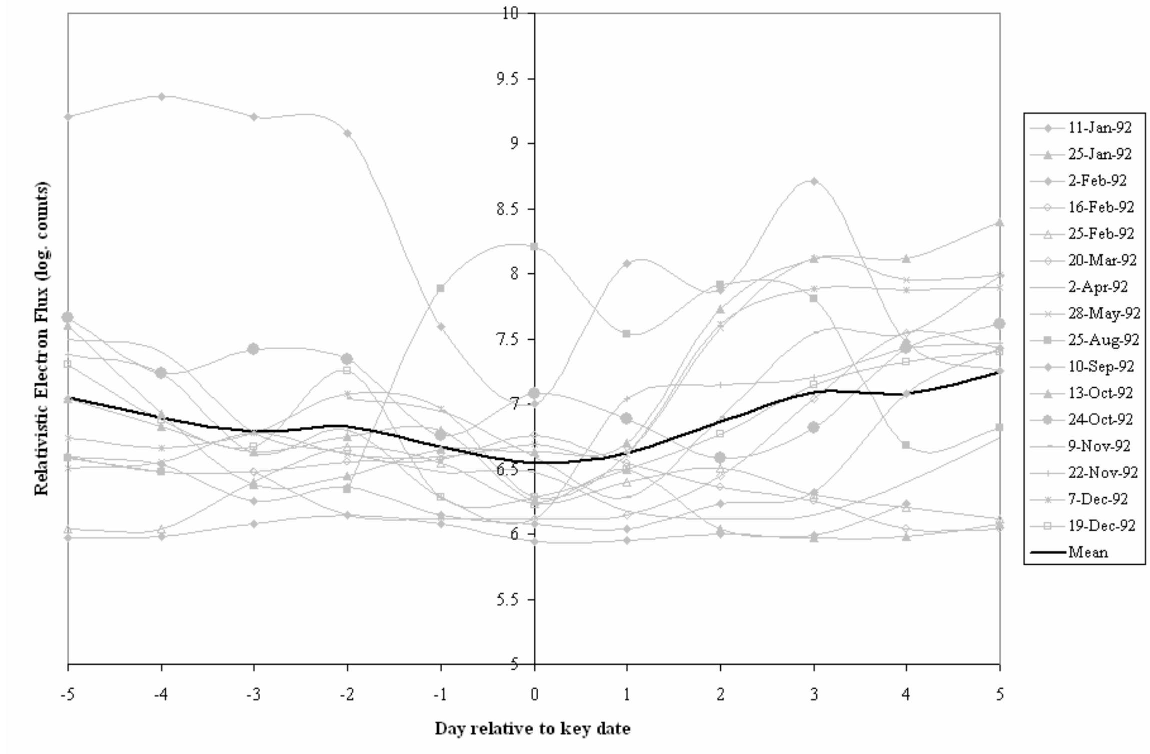

Figures 1a, b, c

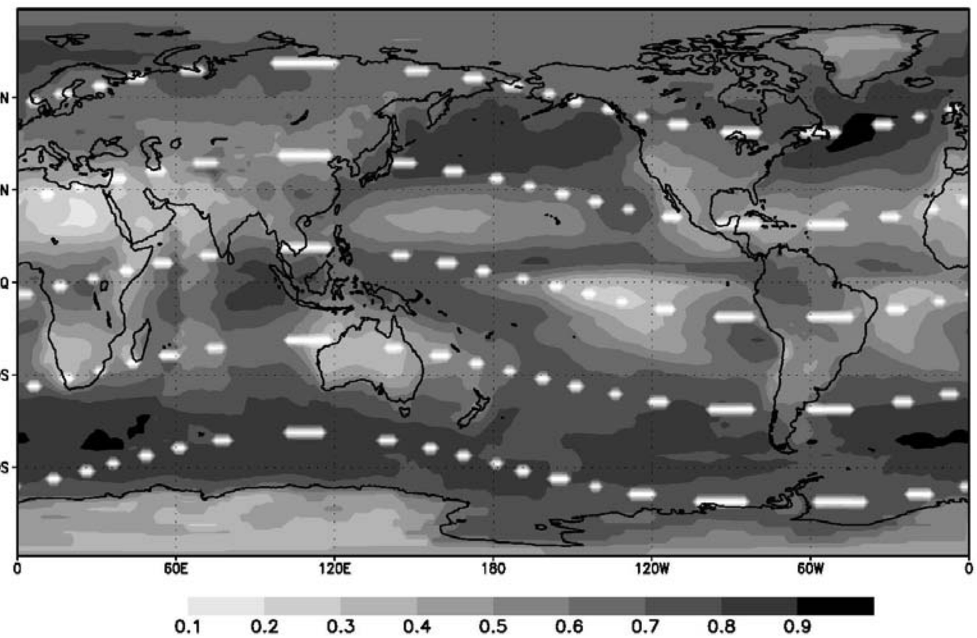
60N
30N
EQ
30S
60S
0
60E
120E
180
120W
60W
0
0.1
0.2
0.3
0.4
0.5
0.6
0.7
0.8
0.9

Figure 2.

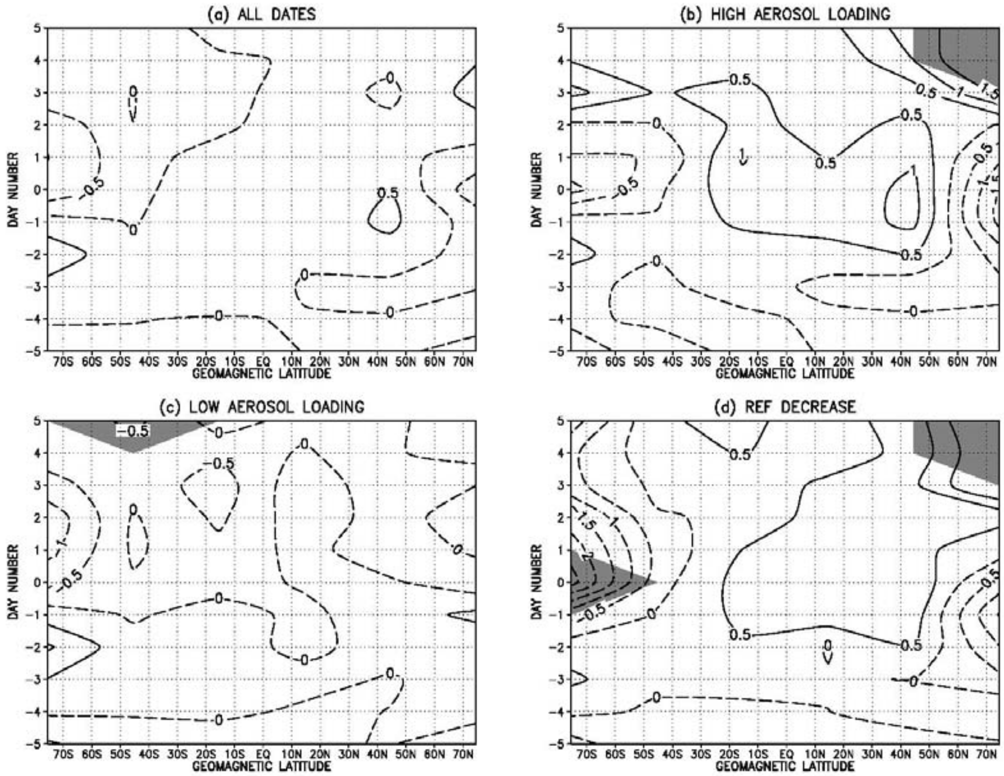
(a) ALL DATES
(b) HIGH AEROSOL LOADING
(c) LOW AEROSOL LOADING
(d) REF DECREASE
DAY NUMBER
GEOMAGNETIC LATITUDE
70S 60S 50S 40S 30S 20S 10S EQ 10N 20N 30N 40N 50N 60N 70N

Figure 3a-d.

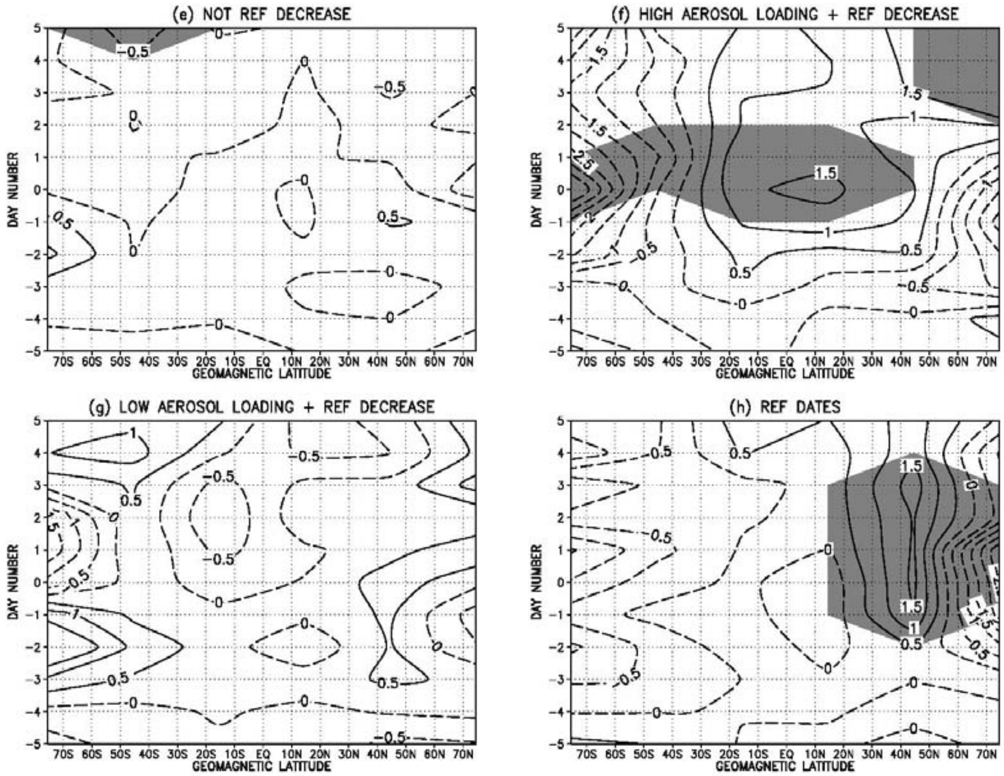

(e) NOT REF DECREASE
(f) HIGH AEROSOL LOADING + REF DECREASE
(g) LOW AEROSOL LOADING + REF DECREASE
(h) REF DATES
DAY NUMBER
GEOMAGNETIC LATITUDE

Figure 3e-h.

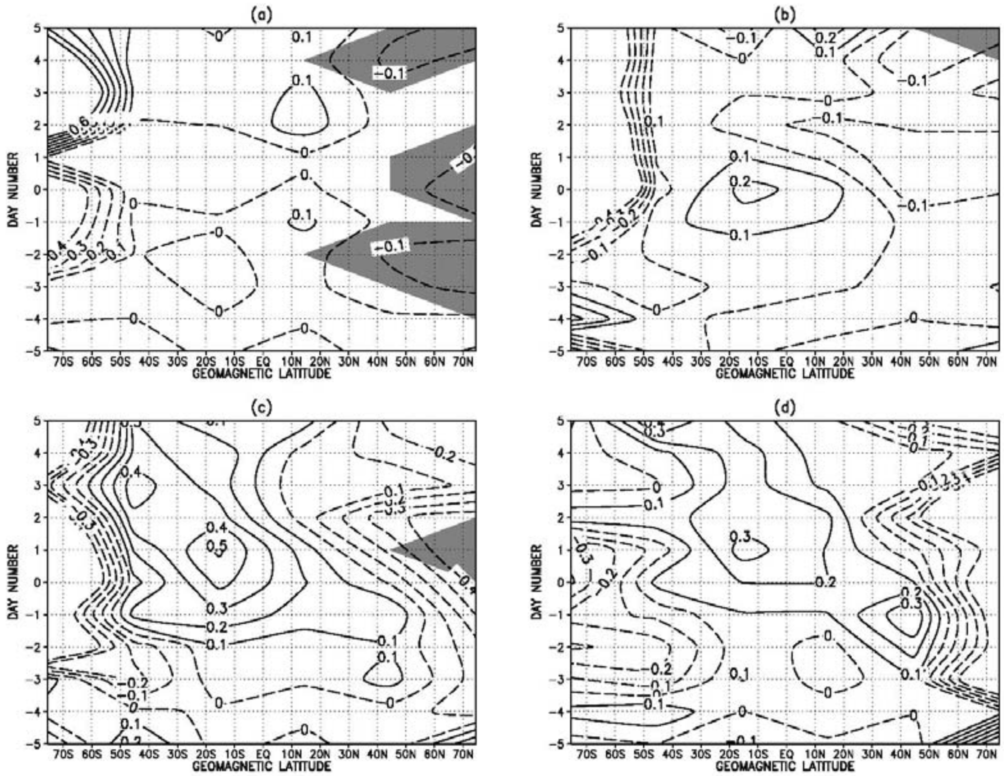
(a)
(b)
(c)
(d)
DAY NUMBER
GEOMAGNETIC LATITUDE
70S 60S 50S 40S 30S 20S 10S EQ 10N 20N 30N 40N 50N 60N 70N

Figure 4a-d.

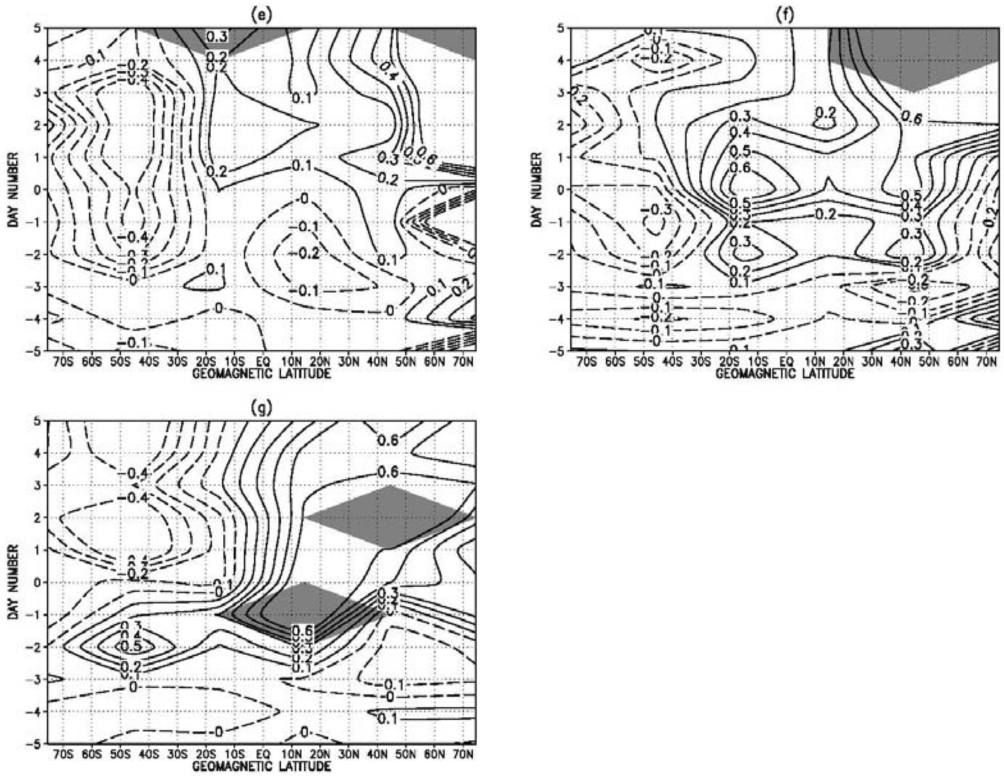
(e)
(f)
(g)
DAY NUMBER
GEOMAGNETIC LATITUDE
70S 60S 50S 40S 30S 20S 10S EQ 10N 20N 30N 40N 50N 60N 70N

Figure 4e-g.

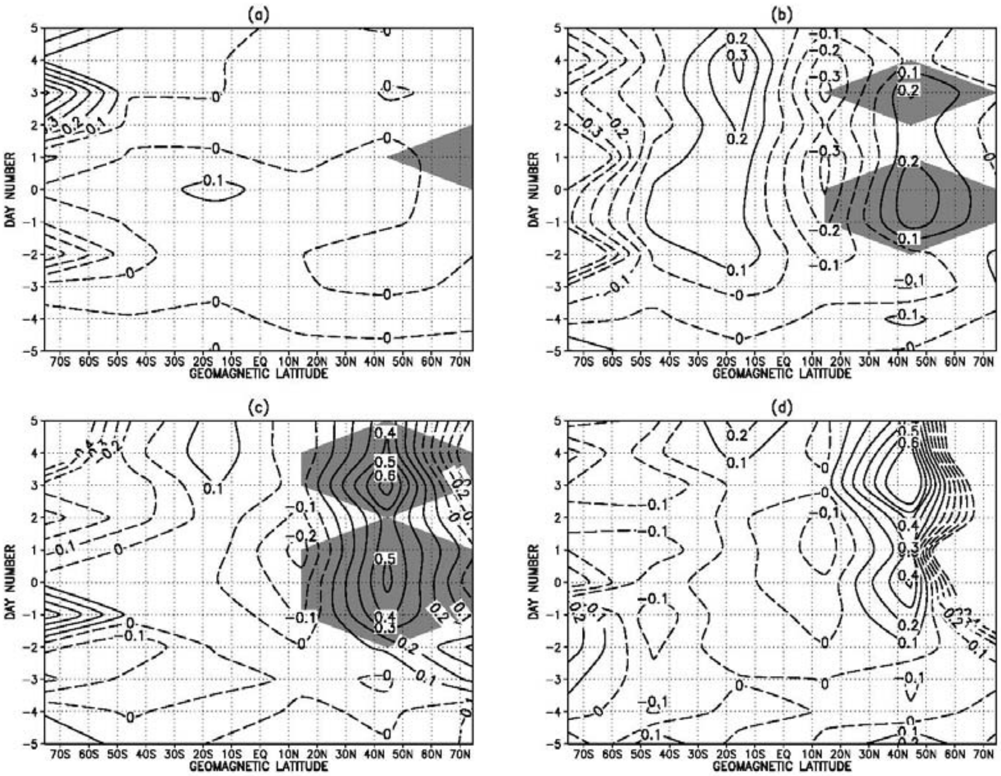

(a)
(b)
(c)
(d)
DAY NUMBER
GEOMAGNETIC LATITUDE
70S 60S 50S 40S 30S 20S 10S EQ 10N 20N 30N 40N 50N 60N 70N
5 4 3 2 1 0 -1 -2 -3 -4 -5

Figure 5a-d.

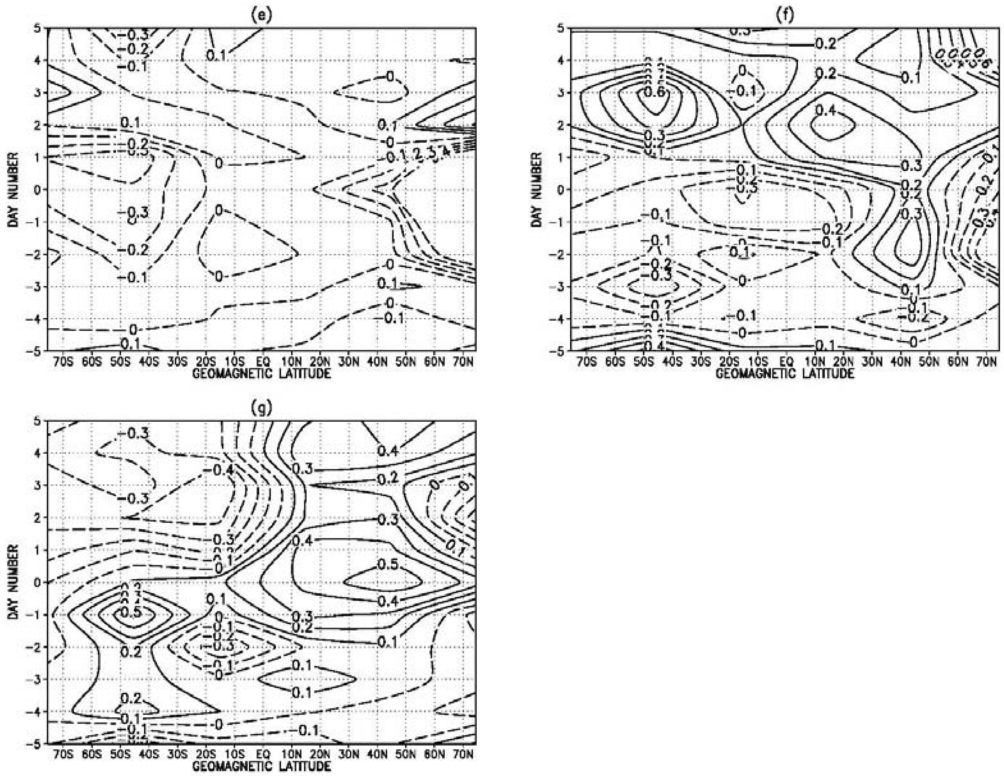
(e)
(f)
(g)
DAY NUMBER
GEOMAGNETIC LATITUDE
70S 60S 50S 40S 30S 20S 10S EQ 10N 20N 30N 40N 50N 60N 70N
5 4 3 2 1 0 -1 -2 -3 -4 -5

Figure 5e-g.

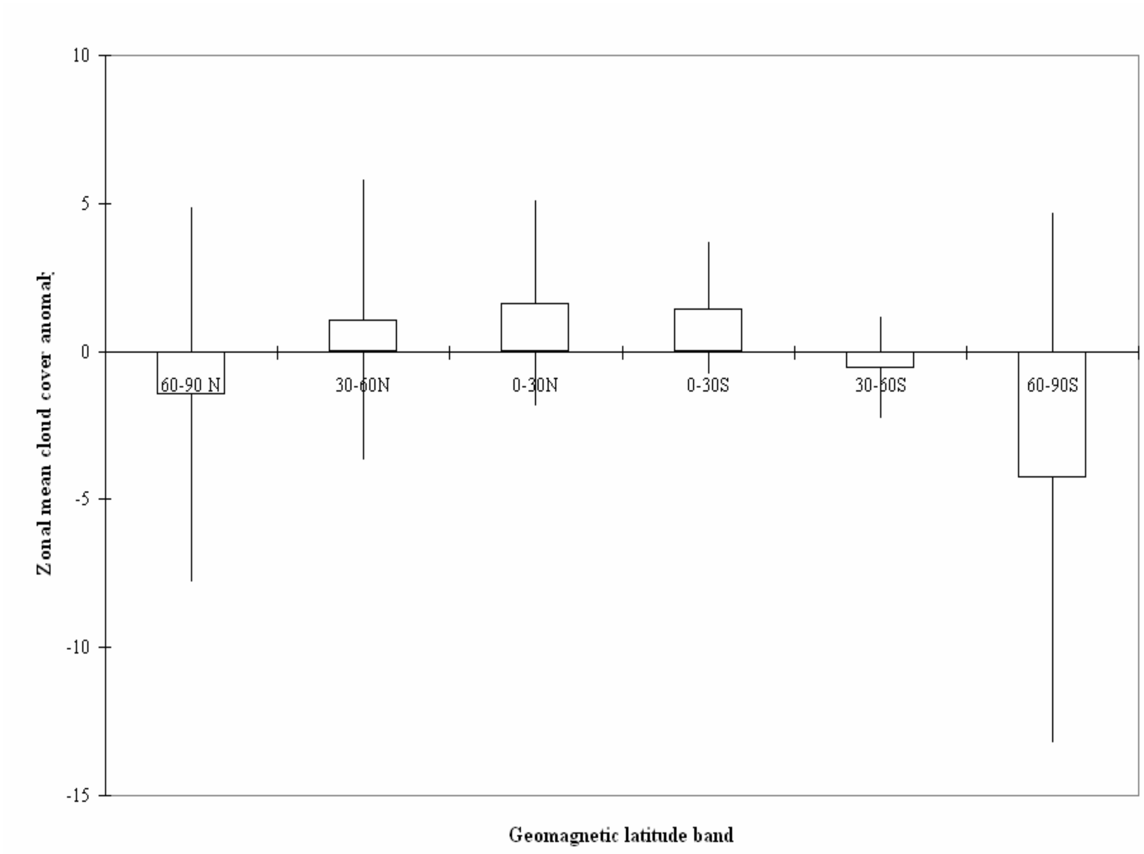
10
5
0
-5
-10
-15
Zonal mean cloud cover anomaly
60-90 N
30-60N
0-30N
0-30S
30-60S
60-90S
Geomagnetic latitude band

Figure 6.